Supporting Information

A novel pH-sensitive (±)-α-tocopherol-5-fluorouracil adduct with antioxidant and anticancer properties

Dong-Wei Li,[a] Fang-Fang Tian,[a] Yu-Shu Ge,[a] Xin-Liang Ding,[a] Jia-Han Li,[a] Zi-Qiang Xu,[a] Mei-Fang Zhang,[a] Xiao-Le Han,[a] Ran Li,[a] Feng-Lei Jiang,[a] and Yi Liu*[ab]

[a] State Key Laboratory of Virology & Key Laboratory of Analytical Chemistry for Biology and Medicine (MOE) & College of Chemistry and Molecular Sciences, Wuhan University, Wuhan 430072, P. R. China.

[b] Department of Chemistry and Life Sciences, Xianning University, Xianning 437005, P. R. China

*To whom correspondence should be addressed:

***E-mail**: yiliuchem@whu.edu.cn; **Fax**: +86-27-6854067; **Tel**: +86-27-68756667*

This section includes:

- Experimental details
  - Materials & Apparatus
  - Free radical scavenging by the DPPH$^{\bullet}$ method
  - MTT assay
  - Fluorescence spectra, UV-visible absorption spectra and circular dichroism (CD) spectra
  - Electrochemical impedance spectroscopy (EIS) experiment
  - Atom force microscopy (AFM)
  - Site marker competitive experiments
  - Molecule docking investigation
- The synthesis of (±)-α-tocopherol-5-fluorouracil (**VE-5-FU**) conjugates
- Quenching of intrinsic fluorescence of SA by **VE-5-FU** or 5-FUA
- The influence of **VE-5-FU** on secondary structure of SA
- The confirmation of binding mechanism and binding number of **VE-5-FU** to SA
- Identification of the binding site of **VE-5-FU** on SA via site marker competitive experiments
- Detailed illustration of H-bond between **VE-5-FU** and Arg218.

Experimental details

Materials & Apparatus. (±)-α-tocopherol and 5-fluorouracil were purchased from Sigma-Aldrich and used without further purification. THF was distilled over Na. 2, 2-Diphenyl-1-picrylhydrazyl (DPPH$^{\bullet}$) was purchased from Alfa Aesar. The solution of bovine serum albumin (BSA), obtained from Sigma-Aldrich, was prepared in PBS (pH = 7.4) based on their molecular weight of 67 000, and stored in a refrigerator at 4 ℃. All other reagents and solvents were of analytical reagent grade. Water was purified by a Millipore system.

All fluorescence spectra were recorded on LS-55 spectrofluorophotometer from Perkin Elmer equipped with 1.0 cm quartz cells and a thermostat bath. The UV-visible absorption spectra were recorded at room temperature on a UNICO 4802 UV-vis Double Beam Spectrophotometer equipped with 1.0 cm quartz cells. CD spectra were measured on Circular Dichroism Photomultiplier from Applied Photophysics Limited, UK. The EIS experiments were performed on a CHI660C electrochemical workstation from Shanghai Chenhua Instrument Company. The MTT assay was performed on Multiscan MK3 from Labsystems, Finland.

Free radical scavenging by the DPPH$^{\bullet}$ method. A freshly prepared solution of DPPH$^{\bullet}$ (100 μM) in ethanol (1 mL) was mixed with a water solution of the pure **VE-5-FU** (1 mL) at different pH or concentration. The mixture was allowed to stand at room temperature in the dark for 5 h and the absorbance at 525 nm was measured at 0, 1, 2, 3, 4, and 5 h with a UV-vis spectrophotometer. From the UV-vis absorption spectra of DPPH$^{\bullet}$ in different solvent (Fig. S1), it was indicated that the emission maximum of DPPH$^{\bullet}$ is slightly red-shifted from 517 to 525 nm as the solvent polarity changed. The remaining concentration of DPPH$^{\bullet}$ was determined from a calibration curve, determined by linear regression (Fig. S2). The actual calibration curve was obtained as follows: $Abs_{DPPH^{\bullet}} = 0.01013\ [DPPH^{\bullet}] + 0.0072$, which is comparable to the calibration curve reported in the literature.[1]

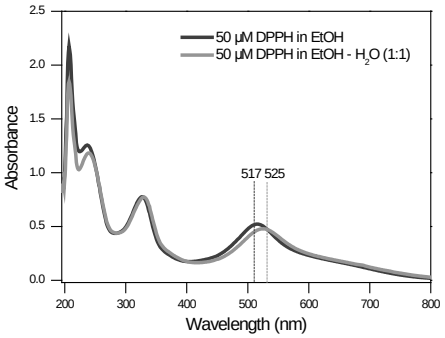

Fig. S1 UV-vis absorption spectra of DPPH$^{\bullet}$ in different solvent.

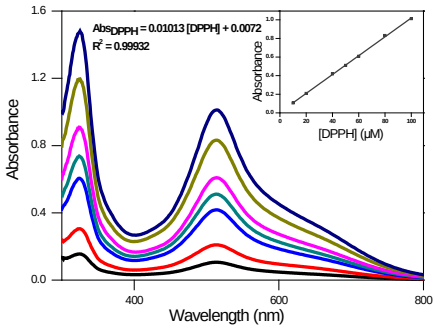

Fig. S2 Absorption spectra of DPPH in EtOH-H_2O (1:1) in the presence of increasing DPPH$^{\bullet}$ concentrations (10, 20, 40, 50, 60, 80, 100 μM). Inset: plot of the absorbance at 525 nm (Abs_{DPPH}) *vs.* [DPPH].

MTT assay. Cells were incubated seeded in 96-well microplate for 24 h at a density of 8×10^3 cells/well at 37 °C and 5% CO_2, and then the growth medium was replaced with DMEM medium containing different concentrations of drugs (**VE-5-FU** and 5-FUA). The drugs stock solutions were prepared by dissolving the drugs in DMSO at different concentrations, then further diluted with DMEM medium to obtain final drugs concentrations of 2.6, 5.25, 10.5, 21, 41.25, 82.5, 165 and 330 μM (final DMSO concentration, 10% v/v). Each sample was prepared in triplicate. After incubation for 48 h, 20 μL of 5 mg/L of MTT solution (in 0.01 M sterilized PBS, pH = 7.4) was added to each well and the plates were incubated for another 4 h at 37 °C under 5% CO_2. After the medium was removed, the plates were added with DMSO (150 μL) and shaken to dissolve the formazan products. Multiscan MK3 microplate reader was used to measure the OD490 of each well. The cell survival rate in the control wells without the drugs solutions were considered as 100% cell survival.

Fluorescence spectra, UV-visible absorption spectra and circular dichroism (CD) spectra. The fluorescence emission spectra were measured at room temperature with a 1 cm quartz cell using 15/4 nm slit widths. The excitation and emission wavelengths for serum albumin (SA) were 280 nm and 350 nm. The emission spectra in absence and presence of 5-FUA or **VE-5-FU** were recorded at 300–500 nm. SA samples (10 μM) were titrated with 5-FUA or **VE-5-FU** by using trace syringe with the final concentration of 5-FUA or **VE-5-FU** in the range of 0–50 μM.

The UV-visible absorption spectra were measured with a 1 cm quartz cell. The wavelength of the spectra was between 200 and 450 nm. The concentration of SA and VE-5-FU were 10 μM.

Circular dichroism (CD) spectra were recorded at room temperature under constant nitrogen flush over a wavelength range of 260–200 nm. Each spectrum was the average of three successive scans and appropriate buffer solutions running under the same conditions were taken as blank and their contributions were subtracted from the experimental spectra. The concentration of SA was kept at 10 μM and the molar ratio of SA to **VE-5-FU** was varied as 1:0, 1:1, 1:2, 1:4 and 1:8. The content of the α-helix, β-sheet and unordered was calculated using SELCON3 and the differential was compared.

Electrochemical impedance spectroscopy (EIS) experiment. **Working electrode preparation** Firstly, the bare gold electrode was polished to a mirror-like surface with 0.3 and 0.05 μm alumina slurry on microcloth pads. Secondly, the working electrode was ultrasonically cleaned in acetone and ultrapure water continuously and then dried by nitrogen airflow. After that, a tiny drop (approximately 5 μL) of SA solution (2 μM) was dropped to the surface of the electrode. After 15 h, the electrode was washed by ultrapure water several times and dried in nitrogen airflow, then ready for use.

Impedance Measurements Impedance measurements were done in a classical three electrode electrochemical testing system: as a working electrode (WE) a gold disk electrode (diameter = 2 mm) modified with SA was used, as a reference electrode (RE) Ag/AgCl electrode was used; counter electrode (CE) was a Pt coil. The electrolyte used in our experiments is a solution of 5×10^{-3} mol·L^{-1} $K_3Fe(CN)_6/K_4Fe(CN)_6$ and 10×10^{-3} mol·L^{-1} KCl at pH 7.4. Active surfaces of WE, RE and CE were contacting with electrolyte and were confined with an O-ring. 10 mL electrolyte was added to an electrochemical cell of 15 mL with a magnetic stirring device. Then, various volumes of **VE-5-FU** solutions were added continuously to the system and stirred for 30 seconds then rest 15 seconds before testing. The EIS were measured with the frequency from 0.1 to 100 000 Hz, and analyzed by a Z-view software to get the R_{ct}. All measurements were repeated three times with different electrodes at room temperature.

Atom force microscopy (AFM). The AFM measurements were performed with a scanning probe microscope "DI Nanoscope Ⅳ" from Veeco, U.S.A. The measurements were carried out in the tapping mode with a silicon nitride cantilever in a triangular shape.

Site marker competitive experiments. Binding studies between **VE-5-FU** and SA in the presence of two site markers (Warfarin and Ibuprofen) were measured using the fluorescence titration methods. The concentrations of SA and Warfarin/Ibuprofen were all stabilized at 10 μM. **VE-5-FU** was then gradually added to the SA–Warfarin or SA–Ibuprofen mixtures. An excitation wavelength of 280 nm was selected and the fluorescence spectra were recorded in the range of 300–500 nm at room temperature.

Molecule docking investigation. The structure of **VE-5-FU** was generated by Sybyl 8.1 package. The molecule structure was optimized in energy and geometry using Tripos Force Field, after being charged using Gasteiger and Marsili method.

The 3D structure of BSA was modeled using Modeller_9v7. The amino acid sequence of BSA was obtained from the NCBI database (http://www.ncbi.nlm.nih.gov/Database/; ID: CAA76847). PDB BLAST of this sequence as query against the protein structure databank identified several structures of human serum albumin (HSA), while the crystal structure of the HSA (PDB entry: 1AO6) had shown the highest homological identity. The model structure of BSA used in this work was modeled according to this crystal structure using Modeller_9v7. The structure was then analyzed by Sybyl 8.1 software, all of the side-chains were repaired, and the bumps were fixed. Polar H atoms were also added. The biopolymer was charged using the AMBER7 FF99 method. The RMS deviation (RMSD) corresponding to equivalent C-α atoms in the BSA model and HSA structure (PDB code: 1AO6) is 0.303 Å. The final structure was used to compute the binding mode of BSA with **VE-5-FU**.

The docking study was conducted by a Surflex-Dock program in the Sybyl 8.1 package.[2-4] The protomol of the binding site was generated by the Residues mode. The threshold was set at 0.50, while the bloat was 6. The parameters in docking work were set as follows: additional starting conformation per molecule: 10; angstroms to expand

search grid: 7; max conformation per fragment: 20; max number of rotatable bonds per molecule: 100; and the ring soft was considered.

The synthesis of (±)-α-tocopherol-5-fluorouracil (VE-5-FU) conjugates

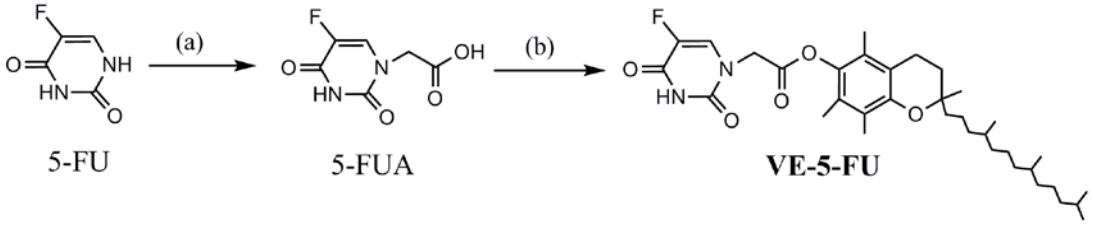

Scheme S1 The synthesis route for **VE-5-FU**. (a): $ClCH_2COOH$, KOH, refluxed, 2h; (b): (±)-α-tocopherol, DCC/anhydrous THF, Ar, 50℃, stirred, 48h.

The synthesis of 5-Fluorouracil-1-acetic Acid (5-FUA**)**: 5-FUA was prepared according to the method reported previously.[5] Briefly, 5-Fluorouracil (5-FU, 3.25 g, 25 mmol) was dissolved in water (30 mL) containing potassium hydroxide (KOH, 2.8 g, 50 mmol), α-chloroacetic acid (2.37 g, 25 mmol) was then added to the solution, and the mixture was stirred at 100℃ for 2 h, keeping pH of the solution 10 by 10% KOH solution. After the reaction, solution was cooled to room temperature (r.t.), hydrogen chloride (HCl) was added to adjust pH to 2, and the resulting precipitate was filtrated. Obtained powder was re-dissolved in a saturated potassium hydrogen carbonate solution, the solution was acidified to pH 2 by HCl, and the resulting precipitate was filtrated (4g colorless needles, 85% yield). **^{1}H NMR** (300MHz, $CDCl_3$, δ(ppm)): 11.95 (s, 1H), 8.09 (d, J = 7.5, 1H), 4.36 (s, 2H).

The synthesis of (±)-α-tocopherol-5-fluorouracil (**VE-5-FU**): To 10 mL of anhydrous THF under Argon atmosphere and constant stirring were added 5-FUA (270 mg, 1.5 mmol), DCC (310 mg, 1.5 mmol), (±)-α-tocopherol (430 mg, 1 mmol). The resulting solution was stirred under Argon at 50℃ in the dark for 48 hours. The reaction mixture was then cooled to room temperature, followed by concentration under reduced pressure. The crude product was purified over an silica column using a ethyl acetate/petroleum ether eluant. A colorless solid (370mg, 60% yield) was obtained. **IR**

（KBr）：3330m；3172m；3042m；2955s；2927s；2851s；1769s；1750s；1728s；1694s；1628m；1575m；1466s；1417s；1376s；1344m；1256s；1246s；1232s；1208s；1187s；1105s；1022s；975m；906w；863m；794s；768w. **^{1}H NMR** (300MHz, $CDCl_3$, δ(ppm)): 8.57 (s, 1H), 4.64 (s, 2H), 2.52(t, J = 7.1, 2H), 2.02(s, 3H), 1.95(s, 3H), 1.91(s, 3H), 1.85-1.65(m, 2H), 1.51-1.47(m, 1H), 1.45-1.43(m, 2H), 1.41-1.27(m, 6H), 1.21(s, 3H), 1.16-0.91(m, 12H), 0.80-0.78(d, J = 6.3, 12H). Mass spectrum: **ESI** (solution in methanol): 633.2 $(M+CH_3OH+H^+)^+$.

Quenching of intrinsic fluorescence of SA by VE-5-FU or 5-FUA

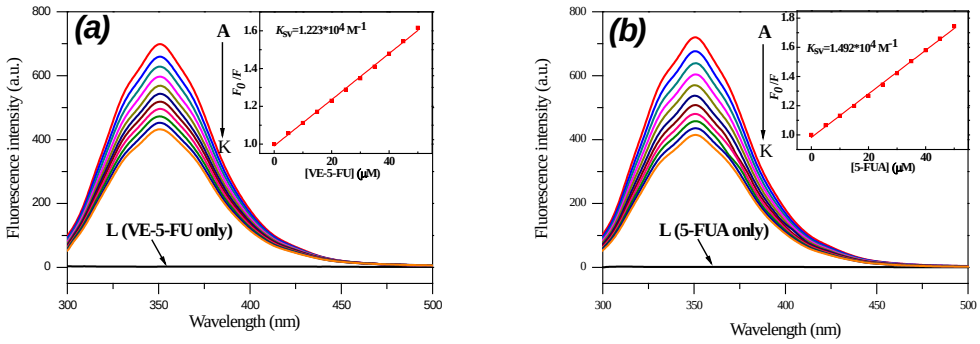

Fig. S3 Fluorescence quenching spectra of 10 μM SA titrated by **VE-5-FU (a)** or 5-FUA **(b)** at r.t.. The final concentrations of **VE-5-FU** or 5-FUA (A─K) were 0, 5, 10, 15, 20, 25, 30, 35, 40, 45, 50 μM. Curve L showed the emission spectrum of **VE-5-FU** or 5-FUA only. The inset corresponded to the Stern–Volmer plot.

The emission spectra of SA in the absence and presence of **VE-5-FU** or 5-FUA were presented in Fig. S3. It was observed that SA showed a strong emission band at 350 nm when the excitation wavelength was fixed at 280 nm, while both **VE-5-FU** and 5-FUA almost gave no emission under the same conditions. The fluorescence of SA was caused by the tryptophan residue excited at 280 nm. The fluorescence intensity of SA decreased regularly and acutely with the increasing concentration of **VE-5-FU** or 5-FUA, which meant that **VE-5-FU** or 5-FUA quenched the intrinsic fluorescence of SA and there existed a binding position near the tryptophan residue between quencher and SA. There was no obvious shift of the maximum emission wavelength, which indicated that the conformation of SA nearly did not change.

The Stern–Volmer quenching constants (K_{SV}), which could be treated as the binding affinity,[6] was obtained by Stern–Volmer equation as follows:

$$\frac{F_0}{F} = 1 + K_{sv}[Q] \quad (1)$$

where F_0 and F are the fluorescence intensities in the absence and presence of quencher, [Q] is **VE-5-FU** or 5-FUA concentration.

From the above equation, the Stern–Volmer quenching constants (K_{SV}) for **VE-5-FU**–SA and 5-FUA–SA system were 1.223 × 10^4 M^{-1} and 1.492 × 10^4 M^{-1}, respectively. It showed clearly that the variation of K_{SV} for **VE-5-FU** compared to its precursor 5-FUA was nearly negligible, which illustrated that the derivatization of traditional anticancer drug 5-FUA had almost no influence on the binding affinity of drug–SA system.

The influence of VE-5-FU on secondary structure of SA

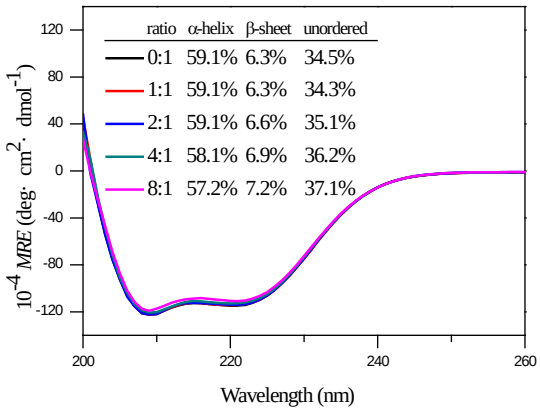

Fig. S4 Effect of **VE-5-FU** on secondary structure of SA. *c* (SA) = 10 μM, *c* (**VE-5-FU**): 0, 10, 20, 40, 80 μM, respectively. The inset corresponded to the contents of α-helix, β-sheet and unordered.

As shown in Fig. S4, **VE-5-FU**–SA displayed the characteristic double negative peaks at 208 and 222 nm, similar to those of SA under native conditions, indicating that the α-helix rich structure was preserved after adding **VE-5-FU**. The contents of β-sheet and unordered calculated by SELCON3 also suggested that the binding of **VE-5-FU** to SA had no significant impact on the secondary structure of SA, and therefore, **VE-5-FU** could be successfully carried by SA without detriment to its function.

The confirmation of binding mechanism and binding number of

VE-5-FU to SA

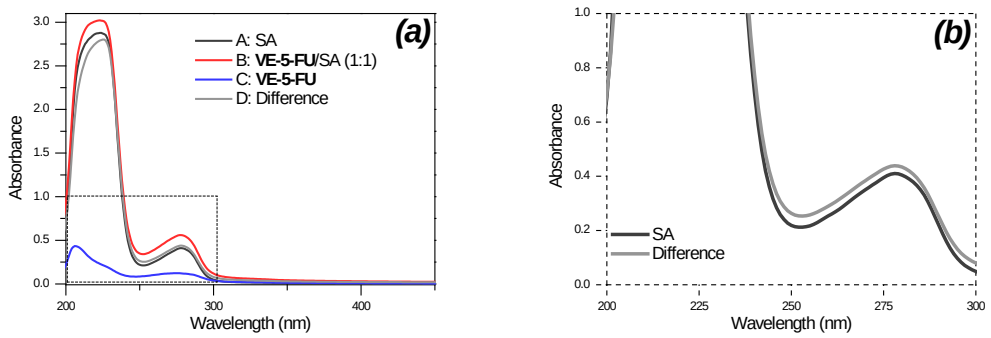

Fig. S5 UV-visible spectra of SA in the presence of **VE-5-FU** at r.t.. **(a)**: A, absorption spectrum of SA only; B, absorption spectrum of **VE-5-FU**/SA 1:1 complex; C, absorption spectrum of **VE-5-FU** only; D, difference between absorption spectrum of **VE-5-FU**/SA 1:1 complex and **VE-5-FU**. *c* (SA) = *c* (**VE-5-FU**) = 10 μM. **(b)**: The absorbance spectra for the wavelength range from 200 to 300 nm.

Classic binding mechanism of molecule to protein can be divided into two kinds: the static binding and the dynamic binding. The former one is primarily caused by the complex formation process, while the latter is largely caused by the collision between molecule and protein. One method to distinguish static and dynamic binding is by careful examination of the absorption spectra of the fluorophore. Collisional binding only affects the excited states of the fluorophores, and thus no changes in the absorption spectra are expected. In contrast, ground-state complex formation will frequently result in perturbation of the absorption spectrum of the fluorophore. For confirming the probable binding mechanism of **VE-5-FU** to SA, we used the difference absorption spectroscopy to obtain spectra, the UV-vis absorption spectra of SA and the difference absorption spectra between **VE-5-FU**–SA and **VE-5-FU** at the same concentration could not be superposed within experimental error (Fig. S5). This result confirmed that the probable binding mechanism of **VE-5-FU** to SA was a complex formation process, rather than a collision process.

In order to assess the binding number of the **VE-5-FU** and SA system, we used the double-logarithmic equation (eq 2) to analyze the fluorescence data.

$$\lg\left(\frac{F_0 - F}{F}\right) = \lg K_b + n \lg[Q] \qquad (2)$$

where F_0 and F are the fluorescence intensities in the absence and presence of the **VE-5-FU**, respectively, and the K_b refers to the binding constant. According to eq 2, a

plot of lg [(F_0 -F)/F] versus lg [Q] will produce a straight line which slope is equal to n, the binding number. For the system of **VE-5-FU** and SA, the value of n at r.t. was obtained to be 1.03, and the linear correlation coefficient was calculated to be 0.9992. The value of n was approximately equal to 1, which indicated that there was one class of binding sites of **VE-5-FU** to SA.

Identification of the binding site of VE-5-FU on SA via site marker competitive experiments

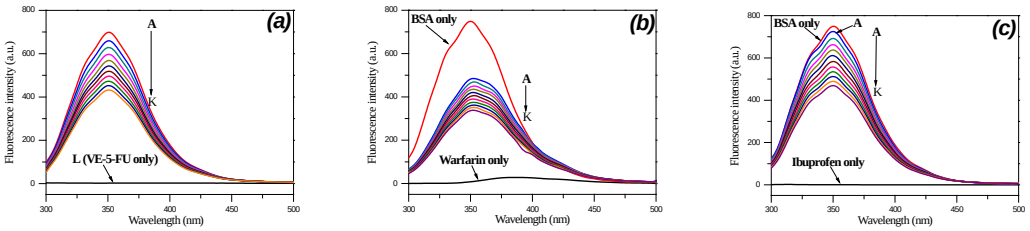

Fig. S6 Fluorescence quenching spectra of **VE-5-FU**–SA system in the absence (a) and presence of site markers warfarin (b) or ibuprofen (c). c (SA) = c (warfarin) = c (ibuprofen) = 10 μM. The final concentrations of **VE-5-FU** (A–K) were 0, 5, 10, 15, 20, 25, 30, 35, 40, 45, 50 μM.

Crystal structure of SA shows that SA is a heart-shaped helical monomer composed of three homologous domains named I, II, III, and each domain includes two sub-domains called A and B to form a cylinder. The principal regions of ligand-binding sites on albumin are located in hydrophobic cavities in sub-domains IIA and IIIA, which exhibit similar chemistry properties. The binding cavities associated with sub-domains IIA and IIIA are also referred to as the site I and site II according to the terminology proposed by Sudlow et al. Warfarin and ibuprofen were used as site marker fluorescence probes for monitoring sites I and II of SA, respectively. In order to identify the **VE-5-FU** binding site on SA, site marker competitive experiments were carried out by using warfarin and ibuprofen which specifically bound to sites I and II on SA.

In the site marker competitive experiments, **VE-5-FU** was gradually added to the solution of SA and site markers held in equimolar concentrations (10 μM). As shown in Fig. S6 b, with the addition of warfarin into SA solution, the maximum emission

wavelength of SA had a slight shift, and the fluorescence intensity was significantly lower than that of without warfarin. Then, with the addition of **VE-5-FU**, the fluorescence intensity of the SA–warfarin (1:1) decreased gradually, indicating that the bound **VE-5-FU** to SA was obviously affected by adding warfarin. By contrast, with the presence of ibuprofen, the fluorescence property of the **VE-5-FU**–SA system was almost the same as in the absence of ibuprofen (Fig. S6 c), which indicated that site II marker ibuprofen did not prevent the binding of **VE-5-FU** in its usual binding location. These results indicated that the binding site of **VE-5-FU** was mainly located within the site I of SA.

Detailed illustration of H-bond between VE-5-FU and Arg218

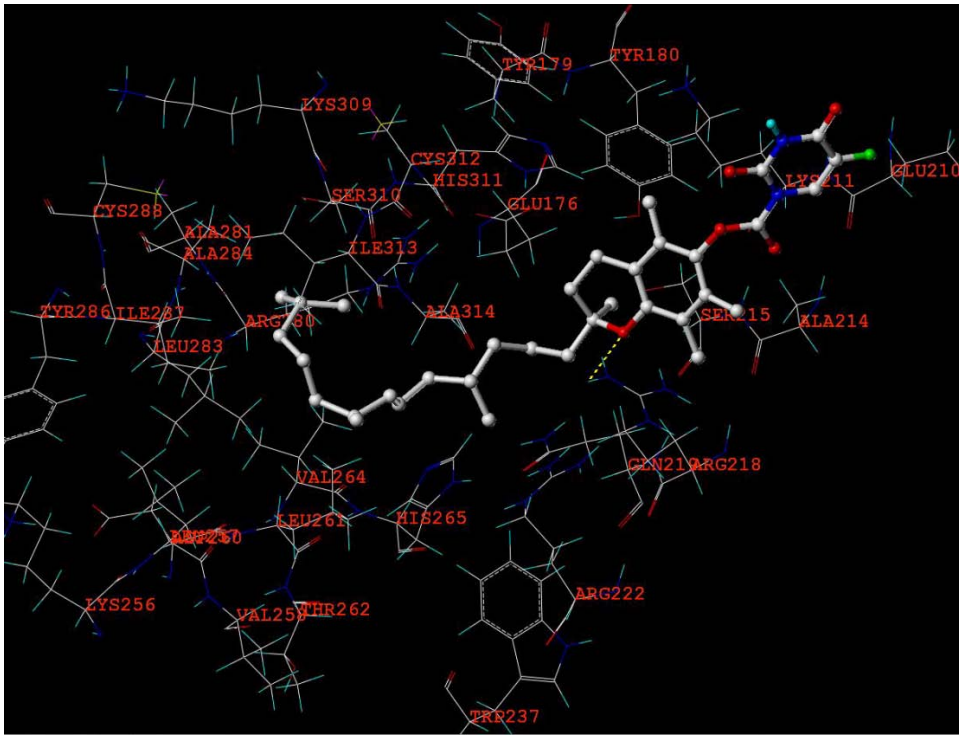

Fig. S7 Detailed illustration of H-bond between VE-5-FU and Arg218. The H-bond (yellow) is highlighted in the figure.

Notes and references

1 P. C. Eklund, O. K. langvik, J. P. Warna, T. O. Salmi, S. M. Willfor, R. E. Sjoholm, *Org. Biomol. Chem.*, 2005, **3**, 3336–3347.

2 A. N. Jain, *J. Med. Chem.*, 2003, **46**, 499–511.

3 T. A. Pham, A. N. Jain, *J. Med. Chem.*, 2006, **49**, 5856–5868.

4 A. N. Jain, *J. Comput. Aided. Mol. Des.*, 2007, **21**, 281–306.

5 M. Tada, *Bull. Chem. Soc. Jap.*, 1975, **48**, 3427–3428.

6 B. Zhou, Z. Zhang, Y. Zhang, R. Li, Q. Xiao, Y. Liu, Z. Y. Li, *J. Pharm. Sci.*, 2009, **98**, 105–113.